Int. J. Electrochem. Sci., 13 **(2018)** 1 – 13, doi: 10.20964/2018.01.16

International Journal of
ELECTROCHEMICAL
SCIENCE
www.electrochemsci.org

Functionalization of Graphene and Dielectric Property Relationships in PVDF/graphene Nanosheets Composites

Xuewen Zheng[1], *Huitao Yu*[1], *Shuangshuang Yue*[1], *Ruiguang Xing*[1], *Qiwei Zhang*[1*], *Yunying Liu*[2], *Bangwen Zhang*[1]

[1] Inner Mongolia Key Laboratory of Ferroelectric New Energy Materials & Devices, School of Materials and Metallurgy, Inner Mongolia University of Science and Technology, 7# Arding Street, Kun District, Baotou 014010, China
[2] School of Chemistry and Chemical Engineering, Inner Mongolia University of Science and Technology, 7# Arding Street, Kun District, Baotou 014010, China
[*]E-mail: zqw8000@imust.edu.cn

Received: 29 August 2017 / *Accepted:* 25 October 2017 / *Online Published:* 1 December 2017

In this paper, a series of the functionalized graphenes, such as graphene oxide (GO), reduced graphene oxide (rGO), carboxylated graphene oxide (GOCOOH), reduce carboxylated graphene oxide (rGOCOOH), fluorinated graphene oxide (GOF), and reduce fluorinated graphene oxide (rGOF), were successfully fabricated, and were introduced into the Poly (vinylidene fluoride) (PVDF) matrix to form composites. The effects of these functional groups on dielectric properties of GO/PVDF composites were systematically investigated. The results show that the reduced functional graphene/PVDF composites (rGOCOOH/PVDF, rGOF/PVDF) exhibit more excellent dielectric properties than that of composite samples without undergoing the reduction reaction (GOCOOH/PVDF, GOF/PVDF). The reduced samples not only possess high dielectric constant, but also maintain lower dielectric loss. And, the rGOCOOH/PVDF composite has better dielectric properties (ε_r = 17.64, tgδ = 0.031) than others, due to strong interfacial and dipolar interactions between PVDF matrix and fillers. These results could be used as a guide to tune dielectric properties of polymer/ graphene composites for their applications in embedded capacitors.

Keywords: Functionalized graphenes; PVDF; Dielectric properties

1. INTRODUCTION

During the past decades, dielectric capacitors have been attracting considerable attention due to their fast charge and discharge capabilities in the power density, which can be applied in many fields, such as embedded capacitors, and high density pulsed-power devices, and so on [1-3]. Generally, a material suitable to practical energy storage device applications mentioned above should have high dielectric constant, low dielectric loss and high energy storage density [4,5]. Compared with inorganic

ferroelectric materials with high dielectric constant, polymers have more excellent flexibility and higher electric breakdown strength, exhibiting potential applications in flexible energy storage devices and embedded capacitors [6]. However, low dielectric constant limits their applications in higher power density devices. In order to avoid this disadvantage, polymers-based composites have been widely considered to be an effective way to improve their dielectric properties [7]. Generally, inorganic nanoparticles or powders with high dielectric constant ($BaTiO_3$ [8], TiO_2 [9], CCTO [10]) are introduced into polymer matrix to improve dielectric performance through two or multi-phase composite effects. Many efforts have been made to enhance their properties by controlling shapes of the fillers and interfaces between fillers and polymers [11]. However, higher filler concentrations (>30 vol%) of inorganic materials are often needed to produce high dielectric constant, which inevitably decreases mechanical properties and processability of composite films, and deteriorates electric breakdown strength and energy storage performance [12]. To achieve excellent flexibility and high dielectric constant, by using polymer-based composites, is up to now still a challenging task.

Recently, another strategy has been widely used to avoid these disadvantages above in ceramic-filled polymer composites films. Namely, electrically conductive materials (carbon nanotubes, graphene and metal nanoparticles, etc.) are incorporated into polymers to form percolated composites with high dielectric properties based on percolation theory, while maintaining excellent flexibility [13]. To date, within different conductive fillers, graphene is one of the most widely exploited and extensively studied materials because of its extraordinary thermal, electric and mechanical properties [14]. Many groups have utilized graphene in the some different kinds of polymer matrixes (PI, PVDF, Expoy etc.) [15]. Ultrahigh dielectric constant of composite films near the percolation threshold, as high as 14000 at 1 kHz, has been reported in many graphene-polymer composites, but very high dielectric loss ($tg\delta>1$) limits their practical applications [16]. To resolve this problem, the chemical functionalization of graphene synthesized using graphene oxide (GO) plays a key role in controlling the dispersion of graphene sheets in polymer matrixes, which not only enhances the compatibility with the polymer matrix but also avoids the direct contact between graphene sheets, thus improving the dielectric properties of composite films. For instance, graphene oxide (GO), reduced graphene (rGO), NH_2-functionalized GO, or carboxyl-functionalized GO were added into the polymer matrix to form composites [17]. Tang et al [18] reported a PVDF/GNS composite with ε_r value of 650 at 2.7 vol% GNS, accompanying by a large dielectric loss. Therefore, how to control chemical functionalization types of GO and interface interactions between two phases are a great challenge to obtain low dielectric loss and high dielectric constant for polymer-based GO composites [19]. In addition, it is still unclear to how to select the optimized functional groups bonded GO to avoid adverse agglomeration of GO while maintaining excellent dielectric properties. Hence, it is necessary to disclose the interaction mechanism between different functional groups of GO and matrix, in order to effectively modulate the dielectric behavior of polymer-based GO composites. Nevertheless, there are relatively few studies to investigate the effects of different functional groups of GO on dielectric properties of polymer composites [20].

According to the concept, a series of the functionalized graphenes, such as graphene oxide (GO), reduced graphene oxide (rGO), carboxylated graphene oxide (GOCOOH), reduced carboxylated graphene oxide (rGOCOOH), fluorinated graphene oxide (GOF), and reduced fluorinated

graphene oxide (rGOF) were successfully fabricated by two-step processes. First, GO mixed with $NaCH_2COOCL$ and NaOH was reacted for 24 h in room temperature to obtain GOCOOH solution. Second, GOCOOH solution was mixed with selectfluor via the Hunsdiecker reaction. The effects of different functional groups on the microstructure and dielectric properties in Poly (vinylidene fluoride) (PVDF) based composite materials were systematically studied.

2. MATERIALS AND METHODS

2.1 Materials

Flake graphite with 392 meshes was purchased from Tengda Co. Ltd (Qingdao, China). Sodium hydroxide (AR grade), potassium permanganate and H_2SO_4 (98 wt%) were bought from Beijing Chemical Factory (Beijing, China). Selectfluor, chloroacetic acid ($ClCH_2COOCH$) and silver nitrate were coming from Aladdin Co. Ltd (AR grade, shanghai, China). Absolute alcohol (AR grade) and N, N-dimethylformamide (SP grade, DMF) were purchased from Tianjin reagents Co. Ltd. Poly (vinylidene fluoride) (PVDF) and Hydrazine hydrate ($N_2H_4.H_2O$) were supplied from Aladdin Co. Ltd (SP grade, Shanghai, China).

2.2 Characterization

Phase structures were identified by X-ray diffractometer (XRD, D8 ADVANCE, BRUKER, Germany) with Cu-Ka radiation. Raman spectra were recorded at room temperature using a HORIBA XploRA system (HORIBA Jobin Yvon Company, Paris, France)) with an excitation wavelength of 523 nm. Fourier transform infrared spectroscopy was measured with an IR spectrophotometer (FT-IR, Bruker IFS66V). Chemical composition and binding energy of samples were conducted by X-ray photoelectron spectra (XPS, Kratos, Axis Supra) equipped with a scanning monochromatic Al Kα (υ = 1486.6 eV). The thermal transition data were obtained with instruments differential scanning calorimeter (DSC, Q600) at rate of 10 °C/min. The dielectric properties (ε_r and tgδ) at different frequencies were characterized by the HP4294A LCR meter (Agilent, Palo Alto, CA). The dielectric constant (ε_r) and loss (tgδ) can be obtained by the following equation:

$$\varepsilon_r = C*d/A \quad (1)$$

$$\text{tg}\delta = \varepsilon_r'' / \varepsilon_r' \quad (2)$$

where C is the capacitance of a capacitor with parallel electrodes, d is the thickness of samples, and A is the active electrode area.. ε_r'' and ε_r' are the imaginary part and real part of dielectric constant, respectively. The electrical field breakdown strength was performed with dielectric strength tester (SLK2674AE, Shanghai shujia Electric Co., Ltd.). The morphology and phase structure were tested by field-emission scanning electron microscopy (FESEM, Hitachi, S4800), and the element mappings were measured by energy dispersive spectroscopy (EDS, OXFORD).

2.3 Synthesis of the rGO, GOCOOH, rGOCOOH, GOF, rGOF

Synthesis of rGO: The rGO was synthesized through two steps. First, graphene oxide (GO) was synthesised by the improved Hummers method [21]. Second, 10 mL $N_2H_4.H_2O$ solution was mixed in 100 mL of the GO (1.5 mg/mL) and reacted for 8 h at 90 °C. Finally, the rGO was obtained after the graphene hydrogel was washed and freeze-dried.

Synthesis of GOCOOH and rGOCOOH: GOCOOH was prepared by the reaction of substitution. First, 100 mL GO (3 mg/mL) was mixed with 10 g $ClCH_2COOCH$ and 10 g NaOH, and stirred for 24 h at 25 °C. Then, the GOCOOH was obtained by centrifugal washing. For the rGOCOOH, the mixture of 10 mL $N_2H_4.H_2O$ solution and 100 mL of the GOCOOH (1.5 mg/mL) was stirred in a water bath for 8 h at 90 ºC. After the obtained graphene hydrogel was washed and freeze-dried, the rGOCOOH was achieved.

Synthesis of GOF and rGOF: GOF was prepared with the Hunsdiecker reaction. 100 mL GOCOOH (3 mg/mL), 0.2 g $AgNO_3$ and 900 mg selectfluor were mixed at 90 ºC for 10 h under Ar gas. During this process, $AgNO_3$ was used as a catalyst. The reacted solution was repeatedly washed with C_2H_5OH and deionized water, the GOF was obtained. Then, the reducing process was followed by adding the mixture of 10 mL $N_2H_4.H_2O$ solution and 100 mL of the GOCOOH (1.5 mg/mL) for 8 h at 90 ºC. Finally, the rGOF was obtained. The prepared processes are shown in Fig. 1.

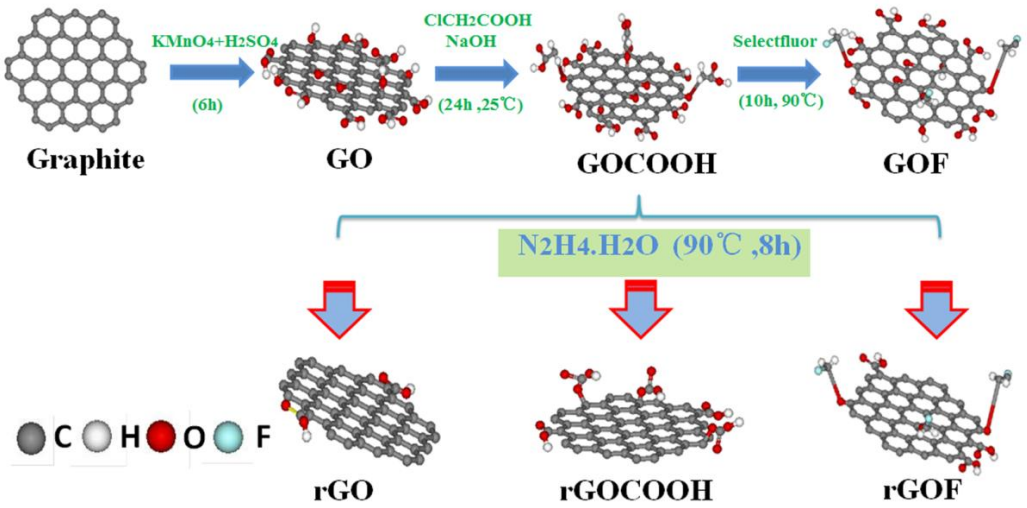

Figure 1. Schematic illustration for preparation processes of different functional graphenes.

2.4 Preparation of composite material

30 mg GO, rGO, GOCOOH, rGOCOOH, GOF or rGOF powders were ultrasonically dispersed in 15 mL anhydrous DMF for 1 h, respectively. Then, PVDF (1 g) was added into the system and stirred for 24 h at 25 ºC. Finally, the mixture (5 mL) was casted on slide glass substrates and dried at 80 ºC for 5 h in a vacuum drying oven.

3. RESULTS AND DISCUSSION

Fig. 2 illustrates the surface and fracture images of the pure GO, rGO, GOCOOH (Fig. S1 (a)), rGOCOOH, GOF (Fig. S1(b)), rGOF and rGOF/PVDF composite. It is clearly seen that these sheets with wrinkled and thin morphology are observed for GO, rGO, rGOCOOH and rGOF samples, and exhibiting typical 2D structure [22]. And these nanosheets are very thin and transmitted by light. In order to certify the compounds, we give the energy dispersive spectroscopy (EDS) of a representative sample (rGOF), as shown in the inset of Fig. 2(d). From which, we found that the F, C or O atoms were uniformly distributed on the surface of rGOF through an efficient decarboxylative fluorination process [23]. From the fractured surfaces of rGOF/PVDF composites (Fig. 2(e) and 2(f)), it is obviously observed that the section is rather smooth, while it is also rough and ridged. These results show that the excellent dispersion of rGOF in PVDF matrix leads to the 2D geometry of graphene sheets.

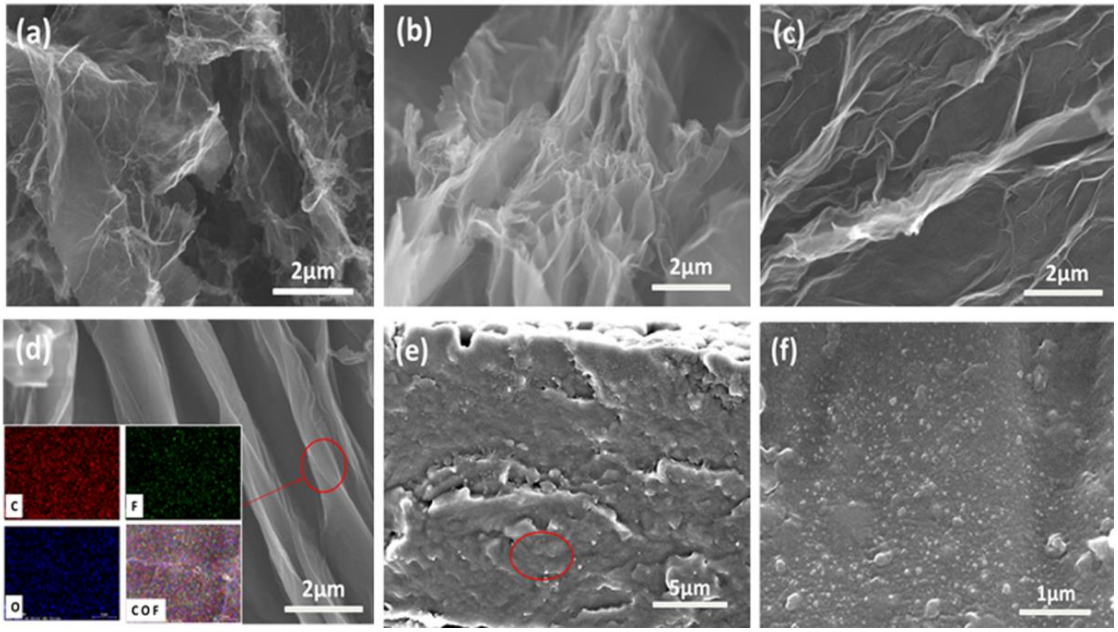

Figure 2. Surface images of the representative samples, (a) GO, (b) rGO, (c) rGOCOOH, (d) rGOF (the insert is the elemental mapping of rGOF, including C, F and O elements), and (e, f) fracture structure images of rGOF/PVDF composites.

FT-IR spectroscopy is used to explain the change of functional groups during the experiment processes [24]. Fig. 3(a) presents the FT-IR spectra of the rGO, GO, GOCOOH, GOF and rGOF samples. All samples show the same absorption bands located at 1080 cm^{-1}, 1723 cm^{-1} and 1418 cm^{-1}, which can be attributed to the -C-O-C stretching of epoxy group, C=O stretching and -C-O stretching of COOH groups, respectively [21]. A broad band at 3425 cm^{-1} represents the -OH stretching of COOH functional groups and the bound water. Compared with other materials, the GOF and rGOF samples have a strong peak located at 1275cm^{-1}, originating from C-F stretching vibration motion [23], which means that the GOF and rGOF sheets have been prepared successfully. Fig. 3(b) shows the TGA results of the samples. The first weight loss occurs at about 180 ºC, which is mainly coming from the pyrolysis of oxygen-containing groups. The weight loss above 250 ºC can be attributed to the slow

removal of the excrescent functional groups. When the temperature is up to 550 ºC, the –COOH groups begin to break down, then leading to significantly increased weight loss rates for the GO, GOCOOH and rGOCOOH samples [21]. Additionally, their weight loss rates (GOCOOH, GOCOOH and GOF) are clearly higher than that of the rGO, rGOCOOH and rGOF samples, indicating that the –COOH and –F groups have been grafted into surfaces of the GO [21,24]. All these results indicate that these materials have been functionalized successfully.

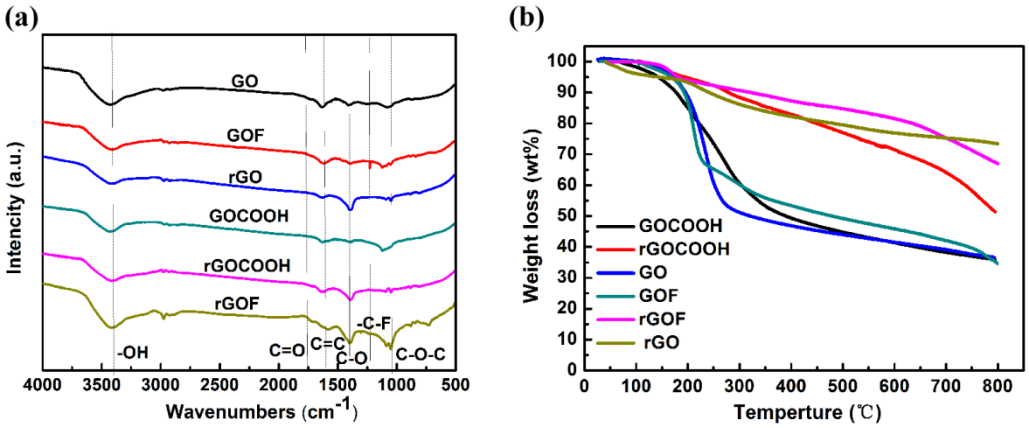

Figure 3. FT-IR (a) and TGA spectra (b) of the GO, rGO, GOCOOH, rGOCOOH, GOF and rGOF samples.

XRD patterns of the samples are shown in Fig. 4(a). According to some reported results, the GO has one main peak at 2θ=10°. After the process of reduction, the rGO has two main peaks centered at 2θ=10° and 2θ=25°, indicating the change of a structure. The characteristic peak (002) of graphite at 2θ=25° indicates a d-spacing of 0.38 nm by the Bragg's equation [25,26]. After chemical oxidation, the basal reflection (002) peak shifts to a lower (2θ=9.8°), indicating a d-spacing of 0.80 nm [27]. The d-spacing widening could could be ascribed to the intercalation of molecules, for example hydroxyl. Compared with the GOCOOH, the GOF has three characteristic peaks at 2θ=28.0°, 32.39° and 46.49°, which can be associated with the d-spacing of 0.316 nm, 0.277 nm and 0.196 nm, respectively, suggesting that the d-spacing of GOF is increased [24]. Moreover, the atomic radius of F is larger than the O, then resulting in the changes in electrical properties of GOF. According to the Raman spectra of samples (Fig. 4(b)), G peak (E_{2g} mode of graphite) at 1575 cm^{-1} and the D band at 1350 cm^{-1} represent the in-plane bond-stretching vibration of sp^2 hybridized carbon atoms and breathing mode of κ-point phonons of A_{1g} symmetric with vibrations of the carbon atoms of dangling bonds in plane termination of the disordered and defected graphite, respectively [21,28]. The variation ratio of the ID/IG is related to the average size of the samples. From Fig. 4(b), it is found that the increase of the ID/IG ratio of GO (0.92) indicates that the excessive oxidation brings about many defects and a high level of disorder [24,28]. At the same time, the rGO (1.17), rGOCOOH (1.2), GOCOOH (0.89), rGOF (1.06) and GOF (1.03) have a higher ID/IG, indicating the introduction of –COOH and –F caused by other equivocal defects. After functionalization process, the D peak gets stronger and broader due to the higher level of disorder.

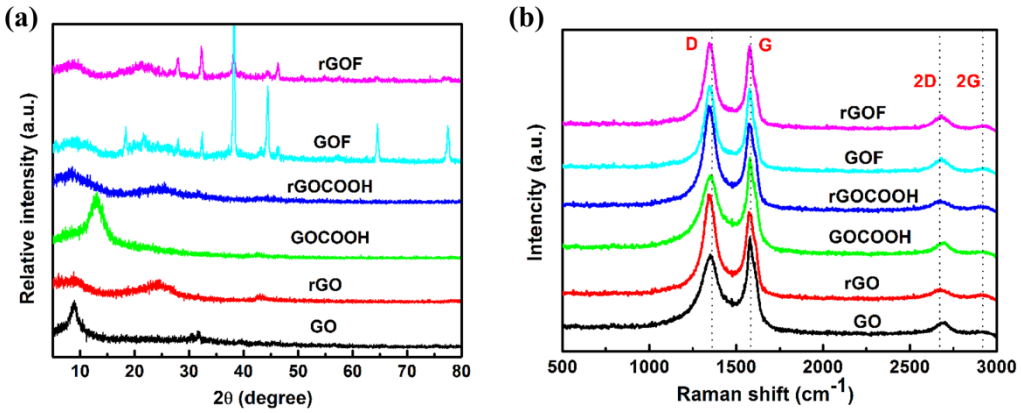

Figure 4. (a) XRD and (b) Raman patterns of the GO, rGO, GOCOOH, rGOCOOH, GOF and rGOF samples.

In order to further investigate surface element compositions and chemical binding of the materials, XPS analyses were carried out. Fig. 5 gives the XPS spectra of C elements for the GO, rGO, rGOCOOH and rGOF samples. The peak intensity of C1s of rGO is higher than other samples, and the O1s of rGOCOOH is higher than others. The presence of F1s in the rGOF indicates that the reduction process and functional treatment are feasible. According to the results from the C1s of GO (Fig. 5(b)), four types of bonded carbon exist in the GO, located at 284.6 eV (C-C/C=C, sp^2 carbon), 286.6 eV (C–O, epoxy/hydroxyl groups), 287.8 eV (C=O, carbonyl groups) and 289.5 eV (O–C=O, carboxyl groups), respectively [21]. For rGO which together with the characteristic C-C, C-N, C=C and C-O/C=O bonds identified from C1s spectra of rGO (Fig. S2, Supporting Information). For the C1s of XPS of rGOCOOH (Fig. 5(c)), there are some new peaks appeared at 284.7, 286.6, 287.1 and 288.5eV, which can be attributed to the C–C, C–O, C=O and O-C=O, respectively [29]. In addition, we found that the relative intensity of the C=O for the rGOCOOH is higher than that of the GO, which means that the GO has a reaction of carboxyl. As shown in (Fig. 5(d)), a C1s profile with main peaks at about 284.6, 285.4, 286.8 and 288.6 eV, corresponding to the C–C, C–O, C=O, and C–F groups, respectively [30]. These results can be also proved by XRD, FT-IR and Raman results mentioned above.

Generally, the modification of interfaces or surfaces of materials plays an important role in tuning dielectric properties of composite materials [31]. Therefore, these functionalized graphenes (GO, rGO, GOCOOH, rGOCOOH, GOF, and rGOF) successfully fabricated are introduced into PVDF matrix to form two phase composites. Fig. 6 presents dielectric properties of PVDF-based composites with different fillers (GO, GOCOOH, rGOCOOH, GOF, and rGOF). The dependences of the dielectric constant (ε_r) and loss (tgδ) of composites materials on frequencies are measured at the frequency range from 1 kHz to 1 MHz and room temperature, as shown in Fig. 6(a) and (b). With increasing frequencies, the dielectric constant of all composite samples gradually decreases, and shows a relatively low change over a wide frequency range [32]. In contrary, the dielectric loss of all samples increases with increasing frequencies. Especially, the dielectric loss remarkably increases when the frequency is above 10^6 Hz.

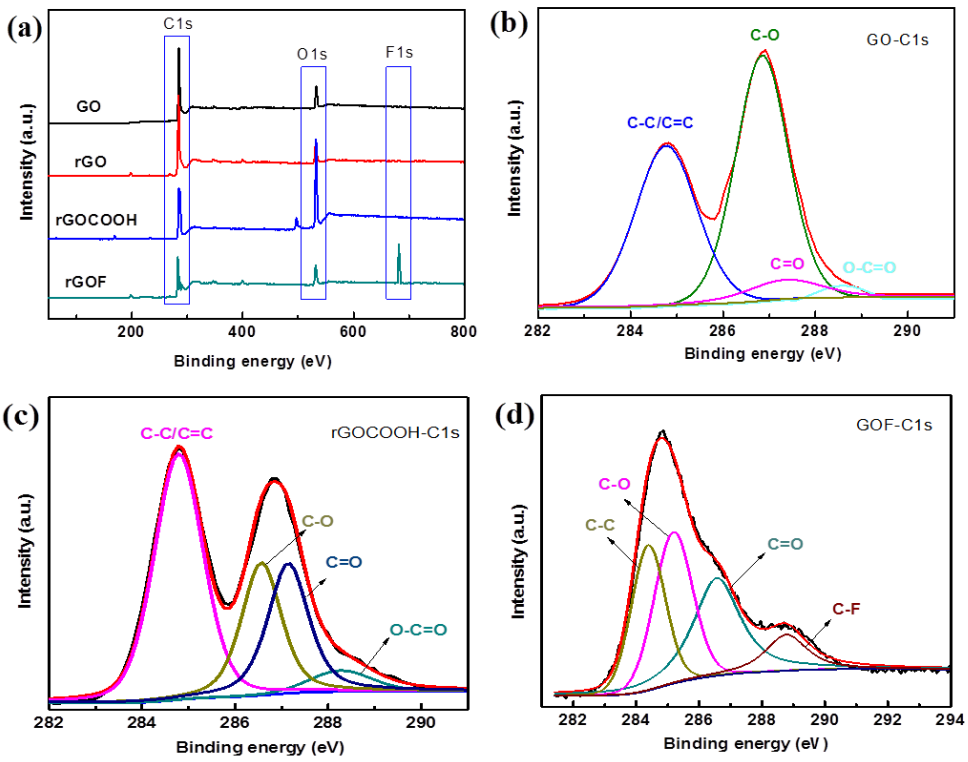

Figure 5. (a) XPS spectra of the GO, rGO, rGOCOOH and rGOF, (b) C1s spectrum of the GO, (c) C1s spectrum of the rGOCOOH, (d) C1s spectrum of the rGOF, respectively.

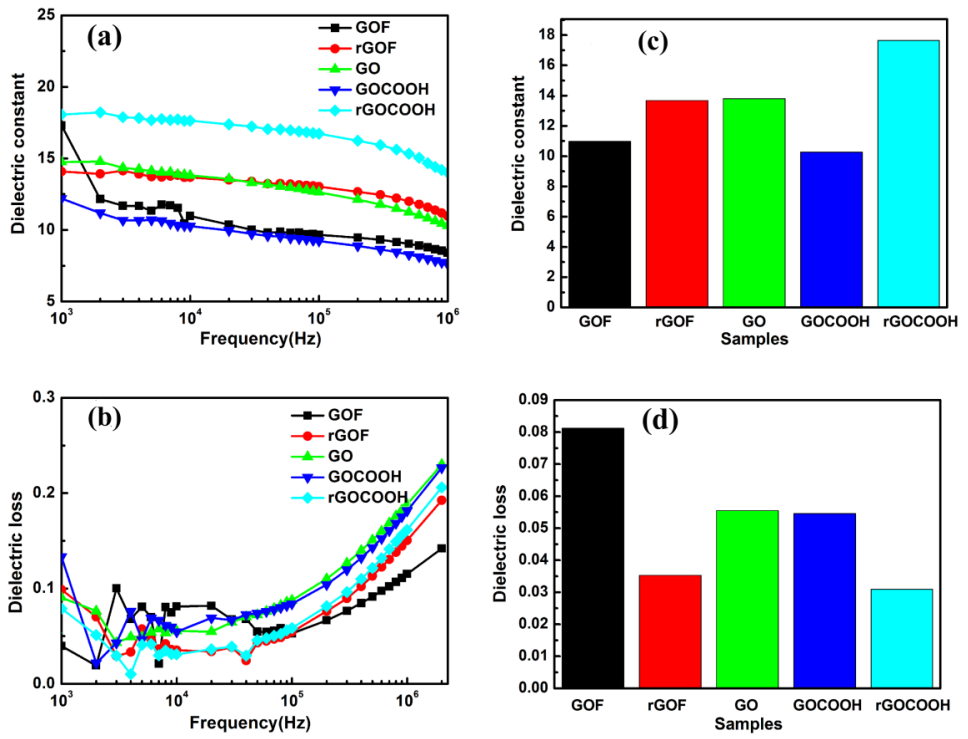

Figure 6. The dependence of the dielectric constant (ε_r) (a, b) and loss (tgδ) (c, d) on frequencies for functionalized graphenes/PVDF nanocomposites at 10 kHz.

Table 1. Dielectric properties of the functionalized graphenes /PVDF nanocomposites at 10 kHz

Sample	ε_r	tgδ (10 kHz)
GOF/PVDF	10.97	0.081
rGOF/PVDF	13.68	0.035
GO/PVDF	13.81	0.055
GOCOOH/PVDF	10.26	0.055
rGOCOOH/PVDF	17.64	0.031
rGO/PVDF	1442.98	0.996

To compare the effects of different functionalized graphenes on the dielectric constant and loss of PVDF composite samples, the dependences of ε_r and tgδ on graphenes with different functional groups at 10 kHz are shown in Fig. 6(c) and (d). Under the similar filler contents (3 wt%), it is clearly demonstrated that the rGOCOOH/PVDF composite sample has relatively higher dielectric constant (ε_r=17.64@10 kHz) than that of other graphene/PVDF composites, and while maintaining a lower loss (tgδ=0.031@10 kHz). Although the rGO/PVDF composite sample possesses ultrahigh dielectric constant (ε_r=1442.98@10 kHz), but the dielectric loss is almost up to 1 (tgδ=0.996@10 kHz) due to the percolation effect (Fig. S3, Supporting Information). Correspondingly, the ε_r and tgδ values are about ε_r=13.81 and tgδ=0.055 for the GO/PVDF, ε_r=10.26 and tgδ=0.55 for the GOCOOH/PVDF, ε_r=10.97 and tgδ=0.081 for the GOF/PVDF, and ε_r=13.68 and tgδ=0.035 for the rGOF/PVDF, respectively (Table 1).

Most importantly, it is found that the reduced functional graphenes/PVDF composites (rGOCOOH/PVDF, rGOF/PVDF) exhibit more excellent dielectric properties than that of composite samples without undergoing the reduction reaction (GOCOOH/PVDF, GOF/PVDF). The reduced samples not only possess high dielectric constant, but also maintain lower dielectric loss [33,34]. For example, for the reduced carboxylated graphene/PVDF (rGOCOOH/PVDF) composites, the ε_r value is about 17.64, obviously higher than the ε_r value of the GOCOOH/PVDF samples (ε_r=10.26), while the tgδ value is about 0.031, lower than the tgδ value of the GOCOOH/PVDF samples (tgδ=0.055). Similar trend is observed between rGOF/PVDF and GOF/PVDF composites. Especially, the dielectric loss is obviously lower than those reported results by other authors. For example, Wu et al. prepared GO/PVDF composite, whose dielectric constant is about 364 with a moderate dielectric loss of 0.077 at low frequency of 1 kHz [35]. Similarly, higher dielectric loss was observed in the expanded reduction graphene/epoxy composites by Yu et al reported with a high dielectric constant of 240 and a dielectric loss of 5 at 1 kHz [36]. Therefore, the only method to effectively decrease dielectric loss is to carry out the functionalization of graphenes, as like reported in present work.

These results discussed above can be well interpreted by a conductive path theory, as shown in Fig. 7. As we all know, surface functionalization of graphenes plays an important role in tuning dielectric properties of composite materials by controlling the dispersion of graphene sheets and interface between two phases [37]. In this paper, the surfaces of GO have been grafted into with

different functional groups (-COOH, -F, and -OH), to effectively avoid the formation of the connectivity path between graphenes (Fig. 7(b)) [24,38]. When these surface-treated GOs (-COOH, -F) are subjected to a reduction process, some parts of functional groups of GOs would be removed, leaving some conductive areas (Fig. 7(c)). These conductive areas would lead to the occurrence of weak conductive paths during the composite process, thus form some so-called "micro-capacitors", which in turn can enhance their dielectric properties in polymer composites, as like some results discussed above [39].

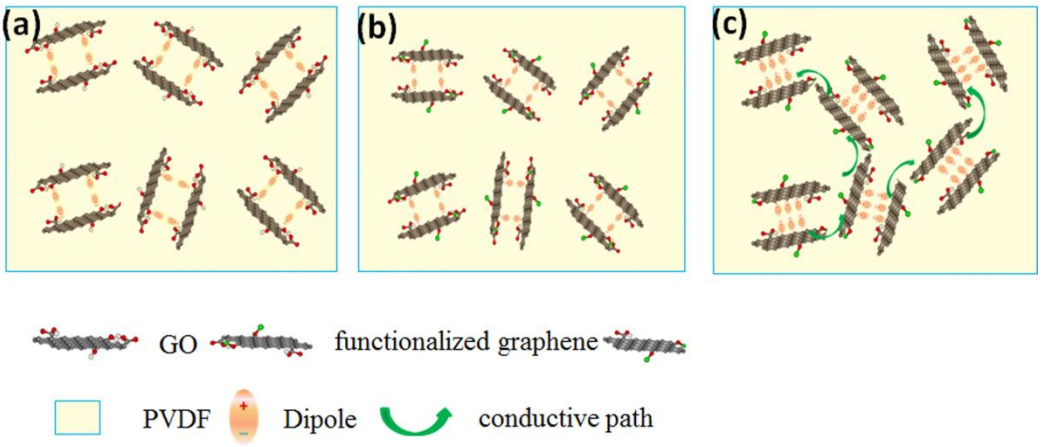

Figure 7. Schematic illustration for the theory of conductive path (a) GO/PVDF, (b) functionalized GO/PVDF, (c) reduced functionalized GO.

The electrical field breakdown strength of composite materials is another important parameter for the practical applications [40]. A two-parameter Weibull distribution can be used to analyze the characteristic electrical breakdown strength (BDS), and the specific formulas are as follows:

$$X_i = \ln(E_i) \quad (3)$$

$$Y_i = \ln(-\ln(1-P_i)) \quad (4)$$

$$P_i = i/(n+1) \quad (5)$$

Where X_i and Y_i are two factors of the Weibull distribution, E_i is the breakdown strength of graphenes/PVDF, n is the total test numbers of sample in the experiment, P_i is the dielectric breakdown at the different condition, and i is the sequence of the materials.

The breakdown strength could be extracted from the fitting lion (Y=0) to obtain the data points [41]. First, the corresponding breakdown field (E_i) and all the other dates are to be listed by numerical size ($E_1 \leq E_2 \leq E_3 \cdots \leq E_i \leq \cdots \leq E_n$). Second, the above data are drawn and fitted. Finally, the BDS of the samples was obtained. As shown in Fig. 8, the electric breakdown strength can be analyzed using a two-parameter Weibull distribution [42]:

$$P(E) = 1 - (-(\frac{E}{E_B})\beta) \quad (6)$$

Where P (E) is the cumulative probability of electric failure, E is breakdown strength, E_B is the characteristic breakdown strength (a scale parameter refers to the breakdown strength at the cumulative failure probability of 63.2%), and β is associated with the linear regressive fit of the distribution.

According to these results, the rGOF/PVDF and GOCOOH/PVDF nanocomposites have higher breakdown strengths than other graphene composites. In addition, it is found that pure GO without undergoing functionalization processes are not suitable to form composites with PVDF matrix for obtaining excellent dielectric properties.

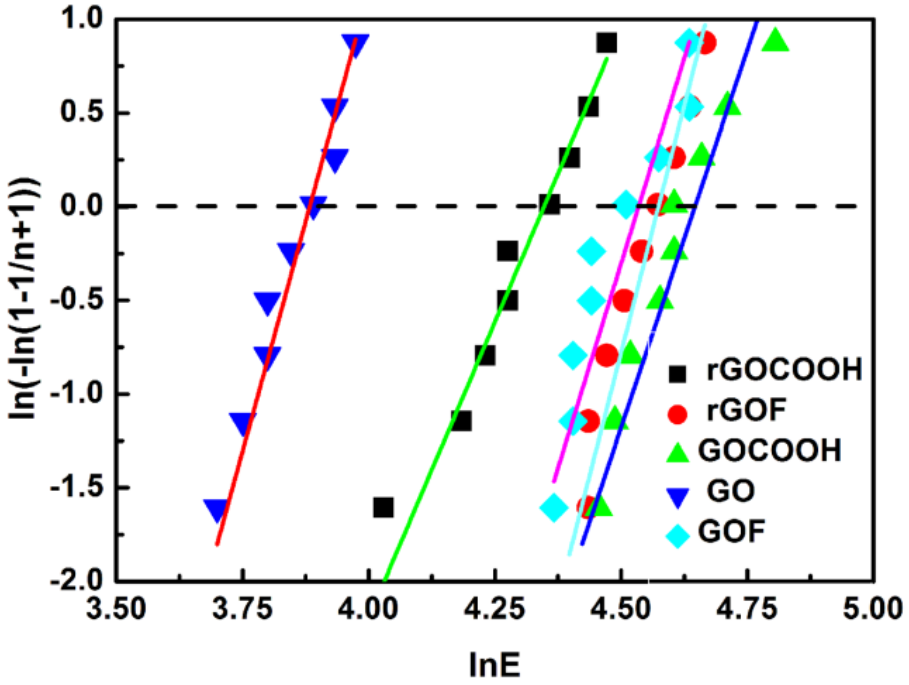

Figure 8. Weibull plots of the electrical strength for functionalized graphenes/poly (vinylidene fluoride) nanocomposites

4. CONCLUSIONS

In present paper, we demonstrated a well-defined way to prepare the different graphenes and fabricated the films of the functionalized graphene/PVDF composites. Meanwhile, the effects of different functional grephenes on dielectric properties of PVDF-based composites were systematically investigated. The rGOF and rGOCOOH/PVDF composites had better dielectric properties than that of the GOF/PVDF and GOCOOH/PVDF samples, such as ε_r=17.64 and tgδ=0.031 for the rGOCOOH/PVDF composite, ε_r = 13.68 and tgδ = 0.035 for the rGOF/PVDF composite. These results discussed above also demonstrate that PVDF-based grephenes composites with high performance can be realized by the structural design.

ACKNOWLEDGEMENTS
This work was supported by the Natural Science Foundation of China (No. 51462028), the Natural Science Foundation of Inner Mongolia (No. 2016MS0208), the Program for Young Talents of Science and Technology in Universities of Inner Mongolia Autonomous Region (NJYT-17-A10).

References

1. R.P. Ortiz, A. Facchetti, T.J. Marks, *Chem. Rev.*, 110 (2009) 205.
2. G. Zhang, X. Zhang, T. Yang, Q. Li, L.Q. Chen, S. Jiang, Q. Wang, *ACS Nano.*, 9 (2015) 7164.
3. X. Fang, X. Liu, Z. K. Cui, J. Qian, J. Pan, X. Li, Q. Zhuang, *J. Mater. Chem. A.*, 3 (2015) 10005.
4. W. Gao, Y. Zheng, J. Shen, S. Guo, *ACS Appl. Mater. Interfaces*, 7 (2015) 1541.
5. B.C. Riggs, R. Elupula, C. Rehm, S. Adireddy, S.M. Grayson, D.B. Chrisey, *ACS Appl. Mater. Interfaces*, 7 (2015) 17819.
6. Z.M. Dang, J.K. Yuan, S.H. Yao, R.J. Liao, *Adv. Mater.*, 25 (2013) 6334.
7. Y. Qiao, M. S. Islam, L. Wang, Y. Yan, J. Zhang, B. C. Benicewicz, C. Tang, *Chem. Mater.*, 26 (2014) 5319.
8. W. Luan, L. Gao, J. Guo, *Ceram. Int.*, 25 (1999) 727.
9. G. Wang, D. Moses, A.J. Heeger, H.M. Zhang, M. Narasimhan, R.E. Demaray, *J. Appl. Phys.*, 95 (2004) 316.
10. E.A. Kafadaryan, K. Cho, N. Wu, *J Appl. Phys.*, 96 (2004) 6591.
11. J. Yu, R. Huo, C. Wu, X. Wu, G. Wang, *Macromol. Res.*, 20 (2012) 816.
12. H. Luo, D. Zhang, C. Jiang, X. Yuan, C. Chen, K. Zhou, *ACS Appl. Mater. Interfaces*, 7 (2015) 8061.
13. N. Yousefi, X. Sun, X. Lin, X. Shen, J. Jia, B. Zhang, J. K. Kim, *Adv. Mater.*, 26 (2014) 5480.
14. V.M. Samoilov, E.A. Danilov, A.V. Nikolaeva, G.A. Yerpuleva, N.N. Trofimova, S.S. Abramchuk, K.V. Ponkratov, *Carbon*, 84 (2015) 38.
15. Y. Wu, X. Lin, X. Shen, X. Sun, X. Liu, Z. Wang, J. K. Kim, *Carbon*, 89 (2015) 102.
16. S. Cho, J.S. Lee, J. Jang, *ACS Appl. Mater. Interfaces*, 7 (2015) 9668.
17. K. Ma, S. Zhang, B. Ye, J. Ouyang, G.H. Yue, *RSC Adv.*, 6 (2016) 29619.
18. H. Tang, H.A. Sodano, *Appl. Phys. Lett.*, 102 (2013) 063901.
19. S. Liu, J. Zhai, J. Wang, S. Xue, W. Zhang, *Acs Appl. Mater. Interfaces*, 6 (2014) 33.
20. G.I. Titelman, V. Gelman, S. Bron, R.L. Khalfin, Y.B. P.H. Cohen, H. Bianco-Peled, *Carbon*, 43 (2005) 641.
21. H. Yu, B. Zhang, C. Bulin, R. Li, R. Xing, *Sci. Rep.*, 6 (2016) 36143.
22. G.I. Titelman, V. Gelman, S. Bron, R.L. Khalfin, Y.B.P.H. Cohen, H. Bianco-Peled, *Carbon*. 43 (2005) 641.
23. H. Touhara, F. Okino, *Carbon*. 38 (2000) 241.
24. R. Xing, Y. Li, H. Yu, *Chem. Commun.*, 52 (2015) 390.
25. J. Parmentier, S. Schlienger, M. Dubois, E. Disa, F. Masin, T.A. Centeno, *Carbon*, 50 (2012) 5135.
26. A.M. Dimiev, J.M. Tour, *ACS Nano.*, 8 (2014) 3060.
27. H.P. Cong, X.C. Ren, P. Wang, S.H. Yu, *Ener. Envir. Sci.*, 6 (2013) 1185.
28. F. Tuinstra, J.L. Koenig, J. Chem. Phys., 53 (1970) 1126.
29. H.U. Lee, H.Y. Yoo, T. Lkhagvasuren, Y.S. Song, C. Park, J. Kim, S.W. Kim, *Biosens. Bioelectron.*, 42 (2013) 342.
30. V. Štengl, S. Bakardjieva, M. Bakardjiev, B. Štíbr, M. Kormunda, *Carbon*, 67 (2014) 336.
31. W. Tong, Y. Zhang, L. Yu, X. Luan, Q. An, Q. Zhang, Z. Zhang, *J. Phys. Chem. C.*, 118 (2014) 10567.
32. M. Tian, Z. Wei, X. Zan, L. Zhang, J. Zhang, Q. Ma, T. Nishi, *Compos. Sci. Technol.*, 99 (2014) 37.
33. L. Qi, B. I. Lee, S. Chen, W.D. Samuels, G.J. Exarhos, *Adv. Mater.*, 17 (2005) 1777.
34. F. Guan, J. Wang, J. Pan, Q. Wang, L. Zhu, *Macromol.*, 43 (2010) 6739.
35. Y. Wu, X. Lin, X. Shen, X. Sun, X. Liu, Z. Wang, J.K. Kim, *Carbon*, 89 (2015) 102.
36. C. Min, D. Yu, *Polym. Eng. Sci.*, 50 (2010) 1734.
37. F. He, S. Lau, H.L. Chan, J. Fan, *Adv. Mater.*, 21 (2009) 710.
38. C. Wu, X. Huang, G. Wang, X. Wu, K. Yang, S. Li, *J. Mater. Chem.*, 22 (2012) 7010.

39. Z.M. Dang, L. Wang, Y. Yin, Q. Zhang, Q.Q. Lei, *Adv. Mater.*, 19 (2007) 852.
40. Z.M. Dang, Y.H. Lin, C.W. Nan, *Adv. Mater.*, 15 (2003) 1625.
41. X. Huang, Y. Li, F. Liu, P. Jiang, T. Iizuka, K. Tatsumi, T. Tanaka, *IEEE Trans. Dielectr. Electr. Insul.*, 21 (2014) 1516.
42. G. Wang, X. Huang, P. Jiang, *ACS Appl. Mater. Interfaces*, 7 (2015) 18017.